IEEE Access
Multidisciplinary | Rapid Review | Open Access Journal

Received December 13, 2017, accepted January 7, 2018, date of publication January 12, 2018, date of current version March 9, 2018.

Digital Object Identifier 10.1109/ACCESS.2018.2792451

An Improved Optimal Sizing Methodology for Future Autonomous Residential Smart Power Systems

UMER AKRAM, (Student Member, IEEE), MUHAMMAD KHALID, (Member, IEEE), AND SAIFULLAH SHAFIQ

Electrical Engineering Department, King Fahd University of Petroleum and Minerals, Dhahran 31261, Saudi Arabia

Corresponding author: Umer Akram (g201512930@kfupm.edu.sa)

This work was supported by the Deanship of Research at the King Fahd University of Petroleum & Minerals under Grant IN161038.

ABSTRACT Accelerated development of eco-friendly technologies, such as renewable energy (RE), smart grids, and electric transportation will shape the future of electric power generation and supply. The power consumption characteristics of modern power systems are designed to be more flexible and easily controllable, which will also affect the sizing of power generation system. This paper presents a methodology for the joint capacity optimization of a typical residential standalone microgrid (MG) employing RE sources, i.e., solar photovoltaic (PV), wind turbines (WTs), diesel generators (DGs), and battery energy storage system (BESS). The MG supplies a residential community load comprising of typical residential load plus electric vehicles (EVs) charging load. The realistic mathematical models of PV, WT, diesel generation system, BESS, and EV load are formulated to improve the capacity optimization methodology, which involves various realistic constraints associated with the RE sources, diesel generation system, BESS, and EV load. The labyrinthine optimization problem is formulated and solved innovatively to 1) minimize the cost; 2) reduce greenhouse gases (GHG) emissions; and 3) curtail dump energy. All three objectives have special significance in designing a standalone MG, for example, cost is related to the economics, GHG emissions deal with global warming, and dump energy is related to the stability and economics of the system. The optimization problem is solved for different possible combinations of PV, WT, DG, and BESS to determine the best possible combination to serve the load effectively and economically. In addition, the impact of load shifting on the sizes of distributed generators and BESS in terms of per-unit cost and GHG emissions is analyzed using the concept of controllable loads. This study could be assumed as a powerful roadmap for decision makers, analysts, and policy makers.

INDEX TERMS Microgrid, optimization, renewable power, electric vehicles, hybrid generation.

NOMENCLATURE

A. ABBREVIATIONS

BESS	Battery energy storage system
DG	Diesel generator
ERBC	Emission reduction benefit cost
ESS	Energy storage system
EV	Electric vehicle
GHG	Greenhouse gases
HPGS	Hybrid Power generation system
MG	Microgrid
PV	Photovoltaic
RE	Renewable energy
WT	Wind turbine

B. INDICES

c	Index of EV class
d	Index of day
e	Index of EV
i	Index of DG
j	Index of year
t	Index of time
m	Index of GHG gases
k	Index of RE sources
l	Index of Storage

C. PARAMETERS

A_{pv}	Area of PV array
c_t	Total number of EV classes

$C_{c,sr}$	Capital cost of RE sources
$C_{c,dg}$	Capital cost of diesel generator
$C_{c,e}$	Capital cost of storage related to energy capacity
$C_{c,p}$	Capital cost of storage related to power capacity
E^{ev}	Battery energy capacity of EV
E_{cc}	GHG emissions correction cost
f_p	Diesel generator fuel cost
$F_{om,v}$	Variable operation and maintenance cost
$F_{om,f}$	Fixed operation and maintenance cost
I	Solar irradiation
M_{dg}	Maintenance cost of diesel generator
n^{ev}	Total number of EVs in each class
n	Total number of intervals
n_{sc}	Total number of renewable sources types
n_{stg}	Total number of storage units
N_{ev}	Total number of EVs
n_{dg}	Total number of diesel generators
n_h	Total number houses
n_l	Total years of operation
N_{pv}^{max}	Maximum number of PV panels
N_{pv}^{min}	Minimum number of PV panels
N_{wt}^{max}	Maximum number of WTs
N_{wt}^{min}	Minimum number of WTs
p^{ev}	Charging rate of EV
p_{min}^{ev}	Minimum charging rate of EV
p_{max}^{ev}	Maximum charging rate of EV
P_{wt}^{r}	Rated power of WT
SOC_c^{min}	Minimum State of charge limit of c^{th} EV
SOC_c^{max}	Maximum State of charge limit of c^{th} EV
T_o	Atmospheric temperature
v_r	Rated speed of WT
v_{ci}	Cut-in speed of WT
v_{co}	Cut-out speed of WT
η_{pv}	Efficiency of PV
η_c	Charging efficiency of battery
η_d	Discharging efficiency of battery
λ	Charge depleting distance of EV
Δt	Time step
$\eth$	Discount rate
φ	Fuel curve intercept coefficient
Ψ	Fuel curve slope coefficient
μ	Cost per unit of PV
σ	Cost per unit of WT
Λ_{ar}	Average arrival time
Λ_{dp}	Average departure time
ρ	EV penetration level
δ	Percentage of EV class

D. VARIABLES

C_h	Total cost of hybrid power generation system
C_b	Total cost of battery energy storage system
C_b	Total cost of diesel generation system
C_{erbc}	Emissions reduction benefit cost
C_{dump}	Dump energy cost
E_s	Energy served
E_{ns}	Energy not served
E_{stg}	Energy capacity of battery storage
E	GHG emissions
E_{BESS}^{min}	Minimum stored energy limit of battery
E_{BESS}^{max}	Maximum stored energy limit of battery
N_{pv}	Number of PVs
N_{wt}	Number of WTs
NDE_s	Net discounted energy served
N_{run}	Total number diesel generator operation hours
p	Life of storage unit
P_{wt}	Power output of WT
P_{stg}	Power capacity of battery storage
P_H	Power output of hybrid generation system
E_{BESS}	Energy stored in battery
P_{BESS}^{c}	Battery charging power
P_{BESS}^{d}	Battery discharging power
P_{DG}	Power output of diesel generation system
p_{dg}	Power output of diesel generator
P_{BESS}	Power supplied by battery
P_L	Load power demand
P_{MG}	Microgrid total power generation
$P_{r,dg}$	Rated power of diesel generator
P_{BESS}^{cmax}	Battery charging power limit
P_{BESS}^{dmax}	Battery discharging power limit
SOC^{ev}	State of charge of EV
T	Time of operation of RE sources
T_o	Atmospheric temperature
v	Wind speed
η	Life of diesel generator
Υ	Dump energy
$\varkappa$	Daily mileage
$\overline{\tau}$	Departure time
$\underline{\tau}$	Departure time
$\hbar$	Energy needed to charge EV
τ^{chg}	Charging time of EV
ξ^{chg}	Hourly charging load of EV

I. INTRODUCTION

Most recently, improving the effectiveness and efficiency of electric energy generation and utilization is a pre-eminent concern around the globe due to number of reasons, i.e., the limited resources of fossil fuels, the legislation of new environmental policies, the increasing effects of global warming, political impacts of energy dependence/independence, and the stochastic nature of renewable energy (RE) sources. Thus, new concepts and novel ideas are being proposed to accomplish this goal. Among them, microgrid (MG) concept has drawn significant attention of both academia and industry for the reliable, efficient, effective, and economical operation of the power system. MGs are state-of-the-art active distribution networks employing distributed generators both renewable and conventional, energy storage systems (ESSs), and variety of loads, operated grid-connected or islanded, in a controlled, coordinated way [1], [2].

MG is a miniature version of the larger utility grid except that, when required, it can be isolated from the main grid to operate in islanded mode [3]. As in MGs, both RE and conventional distributed generators lie in vicinity of the loads, MGs are entrusted to supply the load with more efficient and greener energy, better power quality and reliability, and reduced power losses and network congestion, juxtaposed to the conventional power generation plants. Furthermore, for isolated and remote areas where supplying electricity through national grid is infeasible due to techno-economic constraints, standalone MG that utilizes local available RE sources is considered as a viable attractive alternative and thus adopted in many regions and countries [4]–[7].

The three most widely used RE sources are solar, wind, and hydro, especially solar and wind are getting more attention now-a-days due to, the dramatic reduction in their costs in the past few years and the recent advancements in power electronics which have enabled their easier control, operation, and integration in the power system [8], [9]. Nevertheless, RE sources technologies, i.e., solar photovoltaic (PV) panels and wind turbines (WTs) are dependent on the resources that are random, stochastic, and intermittent as they depend upon weather and climatic changes and time of the day and year. So, the output of PV and WT may not match with the load demand resulting detrimental impact on the reliability of the electric power system.

The problems associated with RE sources for example, poor load following, load mismatch, voltage instability, inferior power quality, frequency deviation, output intermittency, and reliability issues can be potentially addressed by employing suitable combination of the two RE sources technologies (PV and WT) together with the use of an energy storage system, such as battery energy storage system (BESS), as a type of power balancing medium [10]–[16]. It is important to note that the cost of BESS per kilowatt is a strong function of its capacity, and has limited number of life cycles, so supplying a load at 100% reliability by utilizing RE sources and BESS only may result in very high cost. Moreover, the energy stored in BESS depends upon the intermittent RE sources and it may happen during the operation of MG that output of RE sources and BESS become inadequate to supply the load. So, a dispatchable source, i.e., diesel generator (DG) should also be utilized along with the RE sources and BESS to supply a load effectively and economically.

Power output of DG is predictable and independent of climate. However, DG has some disadvantages such as, environmental pollution due to greenhouse gases (GHG) emissions and higher operation and maintenance costs. On the other hand, RE sources and BESS have high initial investment costs, negligible operation and maintenance costs and emit negligible GHG emissions. As too high cost and GHG emissions are prohibitive to commercial and industrial acceptance. So, developing a method for optimizing the sizes and operation of a system, utilizing RE sources, BESS, and DG, to fit application constraints is a crucial task.

Transportation sector has been one of the major contributors of the GHG emissions [17], [18]. The conventional vehicles use fossil fuels, i.e., diesel or gasoline, and emit gases such as carbon dioxide, carbon monoxide, hydrocarbons, and nitrogen oxides. Electric vehicles (EVs) have gained significant attention since the last decade as one of the promising solution for GHG emissions reduction. Continuous advancements in EVs anticipate their massive penetration in the future power system, and the typical load diagram of future power system can be significantly different from the present one without EVs [19], [20]. So, substantial number of EVs must be considered for future power system planning to ensure customers daily travel.

MGs are envisaged to be transformed to smart grids in the future electric power system due to, the innovations in power electronics, and the introduction of the advance high-speed information and communication systems and sophisticated control [21]–[23]. Smart grids are perceived as next-generation power systems, provide two-way communication channels between power generation station and the end user [24], and allow the shifting of load demand away from peak load hours or to renewable generation periods, thereby improving reliability and stability, increasing efficiency, reducing the capacity of peaking generation, which consequently results in several financial, technical, and environmental benefits [25]–[27]. Moreover, the recent increase in the usage of EVs will significantly intensify the load demand, yet at the same time this will improve the pliability of load demand by the control of EVs charging periods and vehicle-to-grid operations [28]–[32]. Owing to these facts, the planning and design of the next-generation power system will not be alike the conventional power system, where all of the involved technologies should be contemplated at the planning and design stage.

In this paper, a capacity optimization methodology is developed for a standalone MG employing distributed generators, i.e., PV, WT, and DG coupled with BESS. The MG supplies a residential community power demand, i.e., typical residential load and EVs charging load. The mathematical models of PV-WT hybrid system, DG system, and BESS are derived to jointly optimize their capacities. Most importantly, mathematical model of EVs load is developed to incorporate this new type of load in the design of power system. The capacity optimization problem involves number of constraints inflicted by PV-WT hybrid system, BESS, DG, and EVs load which complicates the problem. Moreover, the proposed MG design employs both BESS and diesel generation system which require accurate calculations for the BESS cycles and DG operating hours to determine the optimal solution. The optimization problem is formulated and solved innovatively to minimize the cost, reduce GHG emissions, and curtail dump energy. In addition, the effects of load shifting on the cost, GHG emissions, emissions reduction benefit cost (ERBC), and clean energy supplied by the system are also investigated. The proposed idea can be effectively applied for the planning and design of future smart grids.

The simulation results show the effectiveness of the proposed idea.

As a case study, the proposed methodology is validated using real-world data of wind speed, solar irradiation, and residential power demand from Dammam, which is located in the eastern region of Saudi Arabia. The wind power output is calculated using the GE 1.5xle WT power curve characteristics. The EV charging load is simulated by using the real characteristics of different types EVs available in the market.

The remainder of the paper is organized as follows. Section II presents the related work and detailed MG modeling is discussed in Section III. The proposed methodology is demonstrated in Section IV. The information of the databases is provided in Section V. The Section VI presents results and discussions followed by conclusion given in Section VII.

II. RELATED WORK AND RESEARCH GAP

The literature reporting the capacity optimization of RESs, can be divided in two main classes. The first class discusses the sizing of RESs and/or ESSs without considering the smart control of the load demand, and it has acquired much attention in the literature. Reference [33] has proposed a capacity optimization methodology for system employing PV, WT and BESS. The proposed technique is based upon the following key principles: i) high supply reliability, ii) complete usage of the complementary attributes of solar and wind, iii) less fluctuations in the power supplied to the utility grid, iv) BESS charge discharge rate optimization, and v) minimization of the total cost. The sizing of a system utilizing PV, WT, DG, BESS, fuel cell, electrolyzer and hydrogen tank is done in [34]. A multi-objective cost function is developed with the aim of cost minimization, GHG emissions reduction, minimization of unmet load. Particle swarm optimization based approach has been used to solve the multi-objective optimization problem. A multi-criteria decision-making algorithm is presented in [35] for capacity optimization of a PV, WT system, that meets a certain balance of economic, environmental, and social factors. A multi-objective optimization algorithm is developed in [36] for the sizing of a standalone system employing PV, WT, BESS. The sizing is done based upon the power supply reliability, the energy stability, the energy utilization ratio, and the economic efficiency. The non-dominated sorting genetic algorithm is used to determine the optimal size of a standalone system employing PV, WT, and BESS [37]. The optimization problem is solved to achieve minimum cost and maximum reliability. In [38], the capacity optimization of standalone system utilizing, PV, WT, BESS and DG is done based upon three objectives, i.e., i) cost minimization, ii) job creation maximization, and iii) human development index maximization. A pareto-optimization multi-objective evolutionary algorithm is used to solve the optimization problem. The planning of PV, WT, and BESS grid-connected MG is done based upon cost minimization and customer satisfaction maximization, and the optimization problem is solved using mixed integer linear programming [39]. In [40], sizing of PV and BESS is done with the aim of minimization of levelized cost of energy. The proposed methodology also aims to maximize the PV size. A robust optimization approach is proposed in [41] to determine the sizes of PV, WT, ESS supplying energy to a remote telecommunication facility. The aim of the optimization is to minimize the total cost and optimization is carried out using robust mixed-integer linear programming. A methodology for the capacity optimization of a standalone system utilizing PV, WT, BESS, and DG is developed in [42]. Genetic algorithm is used to solve the optimization problem to minimize the life cycle cost, reduce GHG emissions and reduce dump energy. In [43], PSO and fuzzy logic are used to determine optimal sizes and types of distributed generators and optimal capacity of ESS. Similarly, some more methodologies dealing with the capacity optimization of RE sources and ESS are discussed in [44]–[48]

The second class considers the integrating RESs in a smart grid paradigm, where the potential role controllable loads, i.e., EVs and conventional loads for accommodating higher levels of sustainable energy sources are accentuated, for example in [49]–[55]. A stochastic method based upon monte-carlo simulation and particle swarm optimization is developed in [49] for the capacity optimization PV, WT and BESS supplying a smart household load. In [50], a stochastic based optimization methodology is presented for the sizing of PV, WT, BESS. Load shifting plans are developed to give some flexibility and decrease the mismatch between the generation and air conditioning and heating ventilation loads. The optimization problem is solved with the aim of the cost minimization. The effect of several EV control strategies on reducing surplus generation and GHG emissions is studied in [51]. The effects of EVs on high PV penetration levels are investigated in [52]. In [55], capacity optimization of a grid-connected PV, WT and BESS is done based upon the cost minimization.

All the cited studies show that the design of a system employing RE sources and ESS depends upon the behavior of load, solar irradiation, and wind power. It varies from one location to another depending on the local available resources. So, optimal capacities of RE sources and energy storage system calculated for a particular geographical location cannot be taken as optimal for any other location even with same value of peak load demand. Also, most of the system designs in the aforementioned studies are determined based on the cost and GHG emissions. The dump energy that has special significance in the design of RE sources based system is ignored in most of the cases. Ignoring the dump energy at the design stage may lead the system towards the instability especially when the system is stand-alone. We believe that the three main important objectives that should be considered while designing RE based system are i) cost, ii) GHG emissions, iii) dump energy. Cost accounts for the economics, GHG emissions account for environmental policies, and dump energy accounts for stable design and economics. Moreover, a new load type, i.e., EV load has not

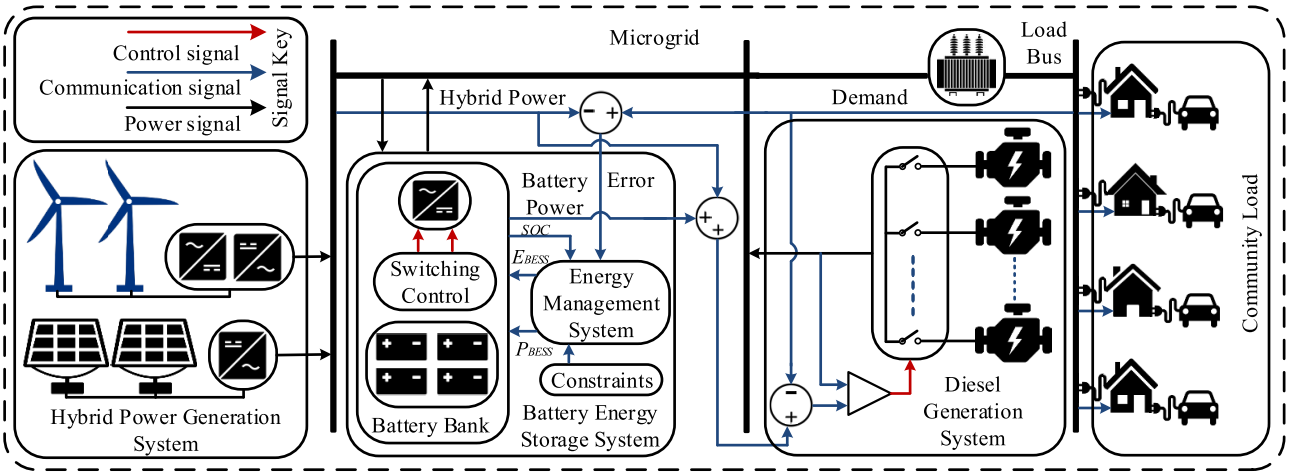

FIGURE 1. A stand-alone MG system.

been considered and modeled properly for the planning of the future power systems. So, novel methodologies are required which incorporate the EVs charging load for the planning and design of power system. In addition, as mentioned earlier that due to the introduction of high speed communication, automation, and sophisticated control, the load demand has become flexible and the load flexibility is expected to increase in future. So, it is also necessary to consider the impact of load shifting on the design of power generation system.

III. MICROGRID MODELING

A stand-alone MG system employing PV panels, WTs, BESS, and DGs to supply a typical residential demand is considered in this study, shown in Fig. 1. The MG system has four major sub-systems: hybrid power generation system (HPGS), battery energy storage system, diesel generation system, and community load demand.

A. HYBRID POWER GENERATION SYSTEM MODELING

The HPGS consists of RE sources, i.e., PV and WT. The PV system is connected to the ac bus via DC-to-AC converter while WT system is connected to the ac bus via AC-to-AC converter. Power output of a solar PV system depends on solar irradiation, area and efficiency of the PV array, angle of incidence, and atmospheric temperature. In this study, it is assumed that a maximum power point tracker (MPPT) is installed to harvest the maximal of available power. Power generated by single PV panel at any instant of time can be calculated using the following equation [56]

$$P_{pv}(t) = \eta_{pv} A_{pv} I(t) \left(1 - 0.005 \left(T_o(t) - 25\right)\right) \quad \forall t > 0 \tag{1}$$

where P_{pv} is the power output of PV system in W, η_{pv} and A_{pv} are the efficiency and area in m^2 of PV panel, T_o is the atmospheric temperature in ^oC, and I is the solar irradiation in W/m^2. Power output of a WT depends upon the wind speed

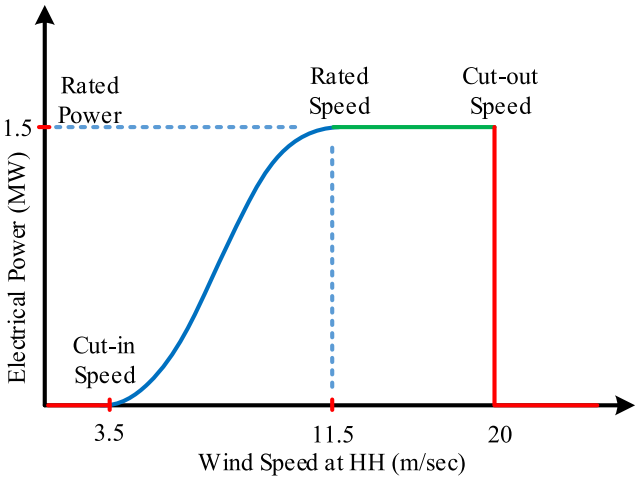

FIGURE 2. Power curve of GE 1.5xle WT.

and hub height (HH). In this study, the characteristics of GE 1.5xle turbine are used to calculate the wind power output. The GE 1.5xle is one of the most commonly used WTs in the industry. Power curve of GE 1.5xle turbine is shown in Fig.2. Power output of the WT is modeled as follows

$$P_{wt}(v) = \begin{cases} 0 & v < v_{ci} \\ \psi(v) & v_{ci} \le v < v_r \\ P^r_{wt} & v_r \le v < v_{co} \\ 0 & v \ge v_{co} \end{cases} \tag{2}$$

where P_{wt} is the power output of WT in W, v is the wind speed in m/sec, P^r_{wt} is the rated power of WT in W, and v_{ci}, v_{co}, and v_r are the cut-in, cut-out, and rated wind speeds in m/sec respectively. From (2) it can be seen that below v_{ci} and above v_{co} WT generates zero power; below v_{ci} power in the wind is not sufficient to either overcome the friction of the drivetrain, or to yield net positive power generation, above v_{co} due to danger of mechanical failure the WT is aerodynamically slowed and stopped, and then mechanically

locked into place to prevent rotation. The total power output of the HPGS is calculated using the equation given below

$$P_H(t) = N_{pv}P_{pv}(t) + N_{wt}P_{wt}(t) \quad \forall t > 0 \tag{3}$$

subject to the following constraints

$$N_{pv}^{min} \leq N_{pv} \leq N_{pv}^{max}$$

and

$$N_{wt}^{min} \leq N_{wt} \leq N_{wt}^{max}$$

where P_H is the total power output of HPGS, N_{pv} is the number of PV panels, and N_{wt} is the number number of WTs.

B. BATTERY ENERGY STORAGE SYSTEM

A BESS consists of series-parallel strings of batteries which are connected to the ac bus via bidirectional DC-to-AC converter. The BESS takes power from the network during surplus generation hours and injects power in the network when needed to improve the efficiency of the system. A BESS model, as given in [56], is formulated as given below

$$Charge:\ E_{BESS}(t+\Delta t) = E_{BESS}(t) + \Delta t P_{BESS}^{c}(t)\eta_c \quad \forall t > 0 \tag{4}$$

$$Disharge:\ E_{BESS}(t+\Delta t) = E_{BESS}(t) + \Delta t \frac{P_{BESS}^{d}(t)}{\eta_d} \quad \forall t > 0 \tag{5}$$

Charging/discharging constraints are

$$0 \leq P_{BESS}^{c}(t) \leq P_{BESS}^{cmax} \quad \forall t > 0 \tag{6}$$

and

$$-P_{BESS}^{dmax} \leq P_{BESS}^{d} \leq 0 \quad \forall t > 0 \tag{7}$$

Stored energy bounds are

$$E_{BESS}^{min} \leq E_{BESS}(t) \leq E_{BESS}^{max} \quad \forall t > 0 \tag{8}$$

where E_{BESS} is the state-of-charge of the battery, P_{BESS}^{c} and P_{BESS}^{d} are charging and discharging powers respectively, and η_c and η_d are charging and discharging efficiency of the battery.

C. DIESEL GENERATION SYSTEM MODELING

As discussed before that the power output of RE sources is unpredictable and variable, so it can happen during the operation of MG that the outputs of the HPGS and BESS become insufficient to supply the required load demand. During such events, the diesel generation system supplies the excessive demand. Instead of a single large DG unit we have assumed several smaller DG units, to enhance the overall efficiency of the system. The power output of diesel generation system is modeled as follows

$$P_{DG}(t) = \begin{cases} \sum_{i=1}^{n_{dg}} p_{dg}^{i}(t) & P_L(t) > P_H(t) + P_{BESS}(t) \\ 0 & otherwise \end{cases} \quad \forall t > 0 \tag{9}$$

where

$$\sum_{i=1}^{n_{dg}} p_{dg}^{i}(t) = P_L(t) - P_H(t) - P_{BESS}(t) \tag{10}$$

where P_{DG} is the total power output of diesel generation system and p_{dg}^{i} is the output power of i^{th} DG unit, n_{dg} is the total number of DGs, P_{BESS} is the power output of BESS, and P_H is the output power of hybrid power generation system. From (9) $P_{DG} = 0$ if power output of RE sources and BESS is more than load power demand.

D. LOAD MODELING

The load can be classified into two main categories: controllable load and uncontrollable load. Every home has some appliances which are devoted to users habits and their needs, for example hair dryers, cooking appliances, refrigerator, computers, and lighting. The load of these appliances is referred as uncontrollable load. In this study, real residential power demand data of Dammam is used.

Similarly, in every home their are some appliances which are controllable, means that shifting their load to some extent do not affect the daily routine of the consumers. For example, water pump, dish washer, clothes dryer, washing machine, and EV, the load of these appliances is called controllable load. Load demand of both controllable and uncontrollable loads except the EV load are incorporated in the load power demand data of Dammam.

In near future, due to the integration of large number EVs in the power system the load demand will increase drastically. Hence, considering the EVs load at the design stage is crucial for the reliable operation of the future power system. Currently the real EVs load is not available. However, EVs load can be approximated. In EV modeling the battery capacity, charge depleting distance, initial SOC, charging/discharging rate, and user behavior are the most important parameters [57]. The battery capacity, charge depleting distance, and charging rate can be acquired in advance. However, the user behavior may not be obtained in advance. In this research, three types of EVs, i.e., Tesla S 70, Nissan Leaf, and Th!nk City are considered to make the analysis more realistic and practical. The information about the battery bank, charging rate, and maximum daily mileage of the three EVs are given in Table 1. The total number of EVs in the system N_{ev} can be obtained from the EV penetration level as follows:

$$N_{ev} = \sum_{c=1}^{c_t} \rho v_c n_h \tag{11}$$

where ρ, is the penetration level, v_c is the percentage of c^{th} class of EV, c_t is the total number of EV classes, and n_h is the total number of houses. The daily mileage, departure time, arrival time, and charging time are different aspects of user behavior which can be obtained from lognormal distribution.

$$\chi_{e,c,d} = logNormal(3.375, 0.5) \tag{12}$$

TABLE 1. Characteristics of EVs.

EV Type	Battery bank (kWh)	Charg./Disch. rate (kW)	Maximum Mileage (mi)
Tesla S70	70	11	240
Nissan Leaf	24	6.6	126
Th!nk City	24	6.6	100

$$\overline{\tau}_{e,c,d} = logNormal(\Lambda_{dp}, \sqrt{3}) \tag{13}$$

$$\underline{\tau}_{e,c,d} = logNormal(\Lambda_{ar}, \sqrt{3}) \tag{14}$$

where $\chi_{e,c,d}$ is the miles driven by the e^{th} vehicle of class c at day d, $\overline{\tau}$ is the departure time, $\underline{\tau}$ is the arrival time, and Λ_{dp} and Λ_{ar} are average departure and arrival times respectively. Once the miles driven are calculated, the energy needed to fully charge an EV can be estimated as described below

$$\hbar_{e,c,d} = \begin{cases} E_c^{ev} & \chi_{e,c,d} \geq \lambda_c \\ E_c^{ev}\lambda_c\chi_{e,c,d} & otherwise \end{cases} \tag{15}$$

where $\hbar$ is the energy needed to charge an EV, E^{ev} is the battery energy capacity of EV, and λ is the charge depleting distance. The time required to charge the EV is modeled as

$$\tau_{e,c,d}^{chg} = \frac{\hbar_{e,c,d}}{p_c^{ev}} \tag{16}$$

where τ^{chg} is total time required to charge the EV and p_c^{ev} is the charging rate of c^{th} class of EV. It is assumed that EVs start charging right after their arrival. The EV charging load is modeled as follows

$$\xi_{e,c,d}\left(\underline{\tau}_{e,c,d} + y\right) = \begin{cases} p_c^{ev} & if\ y \leq \lfloor \tau_{e,c,d}^{chg} \rfloor \\ p_c^{ev}\left(\tau_{e,c,d}^{chg} - \lfloor \tau_{e,c,d}^{chg} \rfloor\right) & else \end{cases} \tag{17}$$

where

$$y = 1, 2, \ldots, \lfloor \tau_{e,c,d}^{chg} \rfloor + 1$$

and

$$\underline{\tau}_{e,c,d} + y > \overline{\tau}_{e,c,d}$$

where ξ is the hourly charging load of EV. The state-of-charge of an EV after charging period is estimated as given below

$$SOC_{e,c,d}(t + \Delta t)^{ev} = SOC_{e,c,d}^{ev}(t) + \Delta t \frac{\xi_{e,c,d}(t)}{E_c^{ev}} \tag{18}$$

where

$$SOC_c^{min} \leq SOC_{e,c,d}^{ev}(t) \leq SOC_c^{max} \tag{19}$$

where SOC^{ev} is the final SOC of an EV after charging. SOC^{min} and SOC^{max} are the minimum and maximum SOC of an EV battery. As EV is a controllable load so its load can be shifted. The shifted EV load is determined as following

$$\xi_{e,c,d}(t + \tau_s) = \xi_{e,c,d}(t) \quad \forall t > 0 \tag{20}$$

subjected to the following shift window constraint

$$\tau_s^{min} \leq \tau_s \leq \tau_s^{max}$$

where τ_s is the time shift. The daily EV hourly load (P^{ev}) can be calculated using following equation

$$P_d^{ev}(t) = \sum_{c=1}^{c_t} \sum_{e=1}^{n_c^{ev}} \xi_{e,c,d}(t) \quad \forall t > 0 \tag{21}$$

We have assumed that MG supplies load of 2000 houses and one EV is assumed for each house. As three different types of EVs are considered is this study so it is assumed that 60% of total number of EVs are Nisaan Leaf, 36% are Th!nk City and 4% are Tesla S70. The percentages of EVs are selected based upon their prices. These percentages can be different for different types of EVs, but this would not affect the methodology.

IV. PROBLEM FORMULATION

One of the primary reasons behind the exploitation of RE sources around the globe is global warming due to GHG emissions. RE sources has proved to be a promising solution for GHG emissions but they have high cost and pose reliability and stability problems in the power system. Hence, in order to get the full benefits of RE sources a system design is necessary, that could significantly reduce GHG emissions at reasonable cost, and should also have higher reliability and stability. The system design in this study is based upon the cost minimization, GHG emissions reduction and dump energy minimization while supplying the load demand reliably.

A. RELIABILITY AND ECONOMIC MODELING

The total power generated by the MG consists of power output of HPGS, BESS, and diesel generation system

$$P_{MG}(t) = P_H(t) + P_{BESS}(t) + P_{DG}(t) \quad \forall t > 0 \tag{22}$$

where P_{MG} is the total generation of MG. Energy served E_s is the sum of the load demand that is supplied by the MG system during its operation, mathematically E_s is defined as

$$E_s = \sum_{t=1}^{n} \Gamma_{es}(t) \tag{23}$$

where

$$\Gamma_{es}(t) = \begin{cases} P_L(t) & P_{MG}(t) \geq P_L(t) \\ P_{MG}(t) & otherwise \end{cases} \quad \forall t > 0 \tag{24}$$

Energy not served E_{ns} is the sum of load demand that is not supplied by the MG during its operation.

$$E_{ns} = \sum_{t=1}^{n} \Gamma_{ens}(t) \tag{25}$$

where

$$\Gamma_{ens}(t) = \begin{cases} P_L(t) - P_{MG}(t) & P_L(t) > P_{MG}(t) \\ 0 & otherwise \end{cases} \quad \forall t > 0 \tag{26}$$

The net discounted energy served NDE_s is calculated as

$$NDE_s = \sum_{j=0}^{n_l} \frac{1}{(1+\eth)^j} E_s \tag{27}$$

where n_l is the total number of years of operation and $\eth$ is the discount rate. The cost of the HPGS is modeled as follows

$$C_h = \sum_{k=1}^{n_{sc}} C_{c,sr}^k P_{sr}^k + \sum_{k=1}^{n_{sc}} \sum_{j=0}^{n_l} \sum_{t=1}^{n} \frac{F_{om,v}^k P^k(t) + T^k(t) F_{om,f}^k P_{sr}^k}{(1+\eth)^j} \tag{28}$$

where C_h is the total cost of hybrid generation system, $C_{c,sr}^k$ is the investment cost of the k^{th} source in $\$/MW$, P_{sr}^k is the installed capacity of k^{th} source in MW, n_{sc} is the total number of sources employed by HPGS, $F_{om,v}^k$ is the fixed operation and maintenance cost of k^{th} source in $\$/MW$, P^k is the power output of k^{th} source, and $F_{om,f}^k$ is the fixed operation and maintenance cost of k^{th} source in $\$/MW-yr$. In (27) the first term represents the initial investment cost and second term stands for the present worth of operation and maintenance costs. The cost of energy storage system depends on both power and energy capacity of BESS. The cost of BESS is modeled as follows

$$C_b = \sum_{l=1}^{n_{stg}} \left(C_{c,e}^l E_{stg}^l + C_{c,p}^l P_{stg}^l \right) + \sum_{l=1}^{n_{stg}} \sum_{s=\ell_{bat}^i}^{n_l - \ell_{bat}^i} \frac{C_{c,e}^l E_{stg}^l + C_{c,p}^l P_{stg}^l}{(1+\eth)^s} \tag{29}$$

where

$$s = \ell_{bat}^i, 2\ell_{bat}^i, 3\ell_{bat}^i, \ldots . n_l - \ell_{bat}^i$$

where C_b is the total cost of the BESS, $C_{c,e}^l$ is the cost related to the energy capacity of l^{th} storage unit in $\$/MWh$, E_{stg}^l is the energy capacity of l^{th} storage unit in MWh, where $C_{c,p}^l$ is the cost related to the power capacity of l^{th} storage unit in $\$/MW$, P_{stg}^l is the power capacity of storage unit in MW, n_{stg} is the total number of storage units, and ℓ_{bat} is the life of the BESS. In (29), the first term stands for the initial investment cost of the BESS, while second term represents the present value of replacement cost of BESS. The cost associated with the diesel generation system is modeled as following

$$C_d = \sum_{i=1}^{n_{dg}} C_{c,dg}^i P_{r,dg}^i + \sum_{i=1}^{n_d} \sum_{s=\ell_{dg}^i}^{n_l - \ell_{dg}^i} \frac{1}{(1+\eth)^s} C_{c,dg}^i P_{r,dg}^i + \sum_{i=1}^{n_{dg}} \sum_{j=0}^{n_l} \sum_{t=1}^{n} \frac{N_{run}^i M_{dg}^i}{(1+\eth)^{j-1}} \left(\Psi^i p_{dg}^i(t) + \varphi^i P_{r,dg}^i \right) f_p \tag{30}$$

where

$$s = \ell_{dg}^i, 2\ell_{dg}^i, 3\ell_{dg}^i, \ldots . n_l - \ell_{dg}^i$$

where C_d is the total cost of the diesel generation system, $C_{c,dg}^i$ is investment cost of i^{th} DG unit in $\$/MW$, $P_{r,dg}^i$ is the rated capacity of i^{th} DG unit in MW, n_dg is the total number of DG units, γ^i is the life of i^{th} DG unit, N_{run}^i is the total operation time of i^{th} DG in hr, M_{dg}^i is the operation and maintenance cost of i^{th} DG in $\$/hr$, f_p is the fuel price in $\$/ltr$, P_{dg}^i is the power output of i^{th} DG, Ψ^i is the fuel curve slope coefficient of i^{th} DG unit, and φ^i is the fuel curve intercept coefficient of i^{th} DG unit. In (30), the first term represent the initial investment cost of diesel generation system, second term stands for the replacement cost, third term represents the present worth of the cost associated with the operation and maintenance costs and fuel cost of diesel generation system.

TABLE 2. Greenhouse gases emission data.

Greenhouse gases	CO_2	CO	SO_2	NOx
Emissions (kg/MWh)	1000.7	1.55	9.993	6.46
Correction Cost ($/kg)	0.0037	0.16	0.97	1.29

B. GHG EMISSIONS MODELING

When electric power is generated by burning fossil fuels, it results in GHG emissions in the environment. There is a correction cost which is needed to mitigate the damage caused by these emissions as shown in Table 2. This correction cost would be a saving if the electric power is generated by utilizing RE sources instead of fossil fuels. This saving is named as emission reduction benefit cost (ERBC), and modeled as

$$C_{erbc} = \sum_{j=0}^{n_l} \sum_{m=1}^{4} \sum_{t=1}^{n} \frac{1}{(1+\eth)^j} P_{MG}(t) E^m E_{cc}^m \tag{31}$$

where C_{erbc} is the total emission reduction benefit cost, E^m is the emission of m^{th} type of greenhouse gas in kg/MW, and E_{cc}^m is the correction cost associated with the m^{th} type of greenhouse gas in $\$/kg$.

C. DUMP ENERGY MODELING

As the outputs of RE sources are uncontrollable and stochastic, it is possible during the operation that the output of RE sources become higher than the load demand and BESS maximum watt capacity. During such events the surplus energy should be dumped for stable operation of MG. The cost of dump energy is calculated using the following equation

$$C_{dmp} = \sum_{t=1}^{n} \sum_{j=0}^{n_l} \frac{1}{(1+\eth)^j} \left(\mu \frac{\alpha}{\alpha+\beta} \Upsilon(t) + \sigma \frac{\beta}{\alpha+\beta} \Upsilon(t) \right) \tag{32}$$

where α is the installed capacity of PV, β is the installed capacity of WT, μ is the cost per unit of PV, σ is the cost per unit of WT, and Υ is the dump energy. For simplicity, it is assumed that the total dump energy is equally coming from WT and PV.

D. COST FUNCTION FORMULATION

Although the problem seems complicated due to coordinated nature of system components, however, every effort has been made to simplify the problem as much as possible, and modeling of the problem was carried out in such a way that it converges towards a standard optimization problem at each step, so that the problem can be solved using standard optimization approaches/tools. For example, an objective function has been described in detail, i.e., the objective of the study is to find an optimal combination of PV, WT, BESS, and DG that must supply the complete load demand with lower cost, lower GHG emissions, and lower dump energy.

$$obj:\ J = \sqrt{\left(J_1(\boldsymbol{X}) + J_2(\boldsymbol{X}) - J_3(\boldsymbol{X})\right)^2} \rightarrow \min \quad (33)$$

$$s.t. \begin{cases} \boldsymbol{g}_\ell(\boldsymbol{X}) = 0 & \ell = 1, 2, , \ldots, m \\ \boldsymbol{h}_\iota(\boldsymbol{X}) \leq 0 & \iota = 1, 2, , \ldots, q \end{cases} \quad (34)$$

where

$$\boldsymbol{X} = \left[N_{PV},\ N_{WT},\ E_{stg},\ P_{stg}, P_{r,dg}\right] \quad (35)$$

The first term in the objective function is the total cost of the MG. The total cost of HPGS (28), BESS (29), and diesel generation system (30) is incorporated in the first term of (33). The second term of the objective function represents the cost of dump energy (32), while the last term represents the GHG emissions that are translated in terms of cost using ERBC (31) concept as discussed in Section IV-B. The equality constraints are represented by $\boldsymbol{g}$ and in-equality constraints are represented by $\boldsymbol{h}$. All system constraints are listed as follows:

The Primary System Constraint (Generation = Demand):

$$P_H(t) + P_{BESS}(t) + P_{DG}(t) - P_L(t) = 0 \quad \forall t > 0 \quad (36)$$

The hybrid generation system constraints:

$$N_{PV}^{min} \leq N_{PV} \leq N_{PV}^{max} \quad (37)$$

$$N_{WT}^{min} \leq N_{WT} \leq N_{WT}^{max} \quad (38)$$

Battery energy storage system constraints:

$$0 \leq P_{BESS}^{c}(t) \leq P_{BESS}^{cmax} \quad \forall t > 0 \quad (39)$$

$$-P_{BESS}^{dmax} \leq P_{BESS}^{d}(t) \leq 0 \quad \forall t > 0 \quad (40)$$

$$E_{BESS}^{min} \leq E_{BESS}(t) \leq E_{BESS}^{max} \quad \forall t > 0 \quad (41)$$

Diesel generation system constraints:

$$\sum_{i=1}^{n_{dg}} p_{dg}^{i}(t) = 0 \quad if:\ P_L(t) \leq P_H(t) + P_{BESS}(t) \quad \forall t > 0 \quad (42)$$

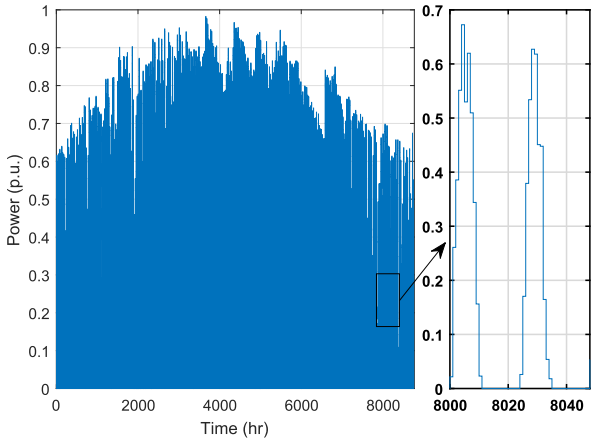

FIGURE 3. Power output of solar power generation system of one calendar year.

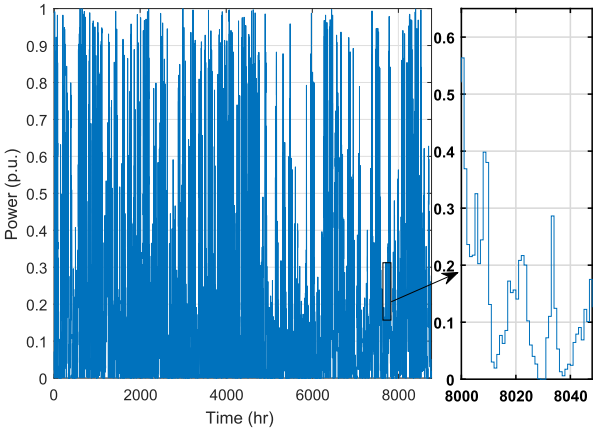

FIGURE 4. Power output of wind power generation system of one calendar year.

$$\sum_{i=1}^{n_{dg}} p_{dg}^{i}(t) = P_L(t) - P_H(t) - P_{BESS}(t)$$
$$if:\ P_L(t) \geq P_H(t) + P_{BESS}(t) \quad \forall t > 0 \quad (43)$$

EV load constraints:

$$SOC_c^{min} \leq SOC_{e,c,d}^{ev}(t) \leq SOC_c^{max} \quad \forall e, c, d, t \quad (44)$$

$$P_{min}^{ev} \leq P^{ev}(t) \leq P_{max}^{ev} \quad \forall t > 0 \quad (45)$$

$$\tau_s^{min} \leq \tau_s \leq \tau_s^{max} \quad (46)$$

V. DATABASES

The solar PV and WT are modeled as discussed in Section III and their power outputs are calculated using the solar irradiation and wind speed data, spanning a length of one year with a resolution of one hour. The power outputs of WT and PV are shown in Fig. 3 and Fig. 4. The solar PV generates power during the day time only and its power increases to maximum from morning to noon and decreasing trend can be observed afterward. The output power of WT fluctuates throughout the day without following any pattern. Similarly, the controllable load is modeled as given in Section III. A community load

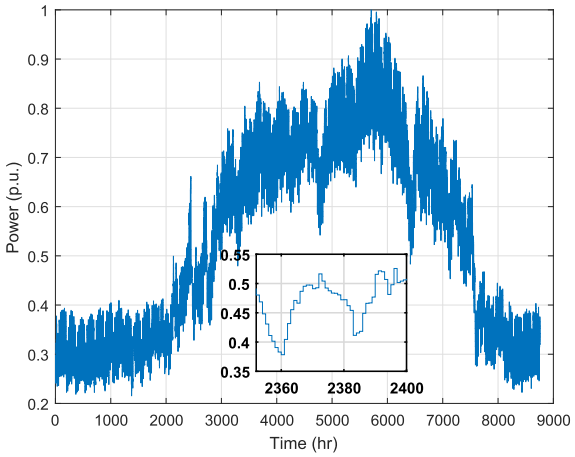

FIGURE 5. Community load power demand spanning a year.

TABLE 3. Economic and technical data of sources [58]–[60].

Parameter	PV	WT	BESS	DG
Investment Cost ($/KW$)	2025	2346	1000, 400*	1521
O & M Cost ($/KWh-yr$)	16	33	10	0.05**
Replacement Cost ($/KW$)	–	–	1000, 400*	1521
Life	20 yr	20 yr	2500 Cycles	15000 hr
DOD	–	–	100%	–
φ, Ψ	–	–	–	0.014,0.244(Ł/hr)

* = $/$kWh$
** = $/$hr$
L = Liter

power demand which consists of EV load and residential load is shown in Fig. 5. The EV owners are expected to reach home around 6 pm, after reaching home the owners start charging their EVs. It can be observed that residential load peak appear around 8 pm. Since, solar PV cannot generate power during the night time, hence supplying this type of load by utilizing RE sources and storage only may result in a very high cost. The tecno-economical data is provided in Table 3.

VI. RESULTS AND DISCUSSIONS

Since the future grid is becoming decentralized, we consider the scenario of an standalone MG. The design of a MG employing RE sources is site dependent and varies from one geographical location to another depending on the local available resources and load demand and their behaviour. Different geographical locations may require different combinations of distributed generators and ESS. So, it is vital to investigate the techno-economical feasibility of different types of available solutions in order to supply the load efficiently and economically. In this study, the following six different topologies for the design of MG are considered:

- CASE-I: PV-WT-BESS-DG based MG
- CASE-II: WT-BESS-DG based MG
- CASE-III: WT-DG based MG
- CASE-IV: PV-DG based MG
- CASE-V: PV-WT-DG based MG
- CASE-VI: PV-BESS-DG based MG

TABLE 4. Optimal capacities of different MG topologies.

Case Index	PV (MW)	WT (MW)	BESS (MWh)	BESS (MW)	DG (MW)
CASE-I	13.86	7	23.76	4.75	10.0
CASE-II	0	10.4	18.53	3.71	10.0
CASE-III	0	8	0.00	0.00	10.0
CASE-IV	11.17	0	0.00	0.00	11.0
CASE-V	10.0	6.04	0.00	0.00	10.0
CASE-VI	23.62	0.0	48.25	9.65	8.00

The capacity optimization of these topologies are done using the cost function as in Section IV-D. The capacities that correspond to the optimal solution are tabulated in Table 4. The cost, reliability (energy served) and GHG emissions have special significance in assessing the performance of a MG employing both RE sources and conventions generators. It is always desired that a system should have lower cost, higher reliability and lesser GHG emissions. The cost per-unit of the six MG topologies is presented in Fig. 6a. The term cost per-unit incorporates both cost and reliability indices in it. It can be seen that per-unit cost is minimum for CASE-I in which all available sources are utilized, while cost is maximum for CASE-IV in which only PV and DG are employed.

As one of the primary purposes behind the utilization of RE sources in the power system is to reduce the GHG emissions by supplying clean energy. The variation in GHG emissions of the six MG topologies is shown in Fig. 6b. The GHG emissions are minimum for CASE-VI as the overall installed capacities of RE sources and BESS are maximum for this case and the DG size is also smallest for this case. While the GHG emissions are maximum for CASE-IV because in this case the only RE source i.e., PV is employed, which supplies the load demand during the day time only, while during the night DG is utilized to supply the demand completely which results in higher GHG emissions. A comparison based on ERBC and clean energy (energy from RE sources and BESS) supplied by the six MG topologies are shown in Fig. 6c and Fig. 6d respectively. The clean energy served and ERBC are maximum for CASE-VI because the overall installed capacities of RE sources and BESS are highest. While ERBC and clean energy supplied are least for CASE-IV.

A MG having lower cost, higher reliability, lesser GHG emissions, higher clean energy, and higher ERBC can be considered as a promising solution. The best topology from the possible solutions is selected by carrying out the sensitivity analysis based upon the per-unit cost, GHG emissions, ERBC, and clean energy served by the system. When comparing CASE-I and CASE-II, it can be observed that

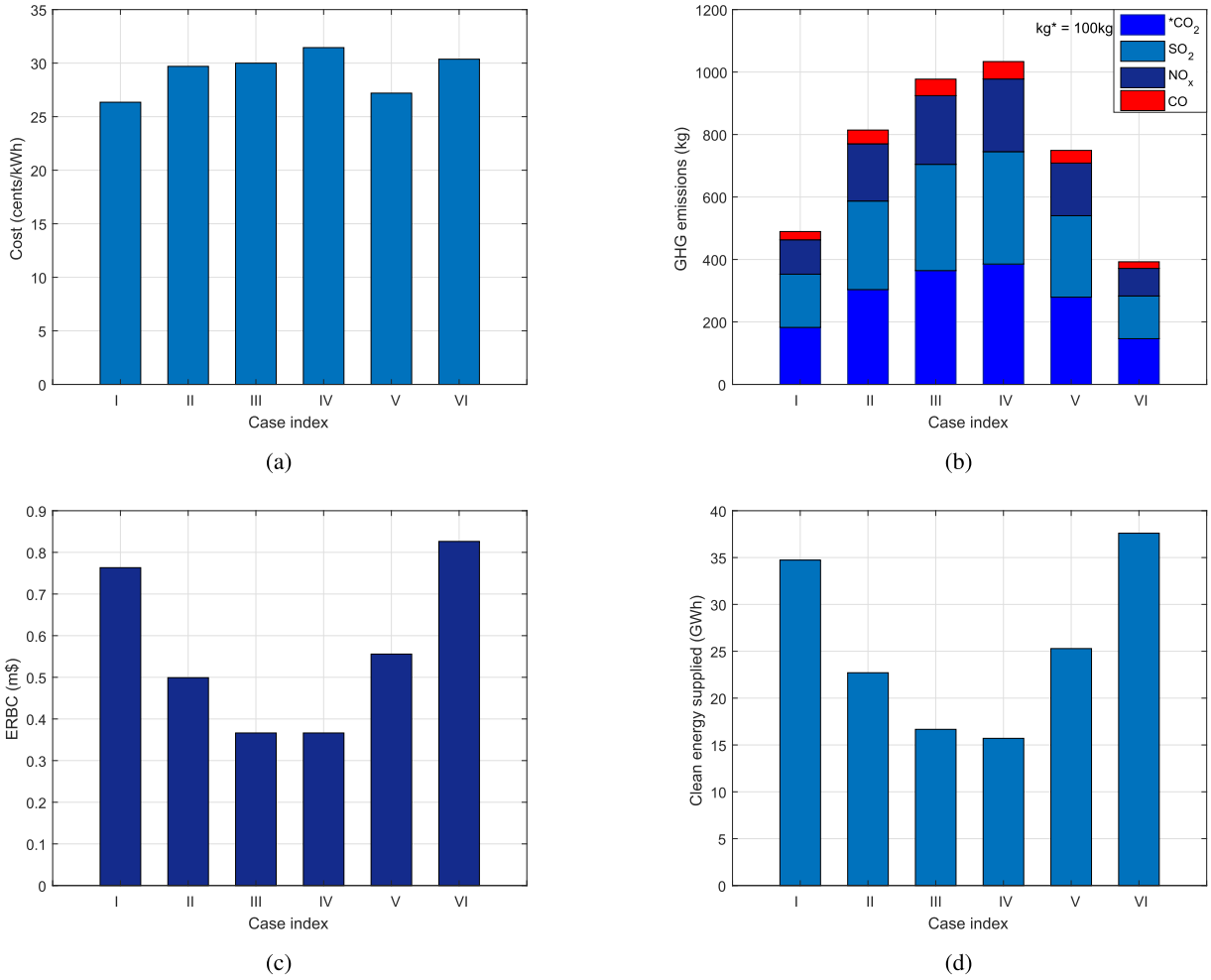

FIGURE 6. (a) Cost per-unit of the six MG topologies (b) GHG emissions comparison of the six MG topologies (c) ERBC comparison of the six MG topologies (d) Clean energy served by the six MG topologies.

CASE-I has lower cost, lower GHG emissions, higher ERBC and higher clean energy which make CASE-I a better solution as compared to CASE-II. Similarly, the cost and GHG emissions are lower and ERBC and clean energy are higher for CASE-I as compared to CASE-III, CASE-IV and CASE-V. The GHG emissions for CASE-VI are lesser than CASE-I but its cost is significantly higher. Hence, from the previous analysis it can be concluded that CASE-I is the better option. It is important to note that these results can not be generalized for any location. As mentioned earlier, the design of a MG exploiting conventional and RE distributed generators is site dependent. Hence, before installing distributed generators, a feasibility study of several possible solutions should be carried out to determine the best techno-economical solution.

The innovations in power electronics and the introduction of the advance high-speed information and communication technologies and sophisticated control has made the load demand of the power system more flexible and easily controllable. In order to highlight the impact of load shifting on the cost, GHG emissions, ERBC, clean energy supplied by the system, the load demand is shifted. The cost function for the MG topology given in CASE-I is solved for different load shifts and the optimal capacities determined are tabulated in Table 5. As the load has typical residential load behaviour due to which peak demand appears in the evening time and shifting the load towards the day time results in a decrease in capacities of DG.

The variation in cost per-unit with the load shift is shown in Fig. 7a. The cost per-unit is minimum for the shift -3 hours and maximum for the shift of 3 hours. Shifting the load by -3 hours results in the efficient utilization of BESS and RE sources which resulted in lower cost. The variation in GHG emissions with the load shift is shown in Fig. 7b. The GHG emissions are lowest for a load shift of 3 hours as for this case the installed capacity of RE sources and BESS are highest, similarly the GHG emissions are also lower for the load shift of -1 hour. The variations is ERBC and clean energy served are shown in Fig. 7c and Fig. 7d respectively. Both ERBC and clean energy supplied are maximum for a shift of 3 hours and

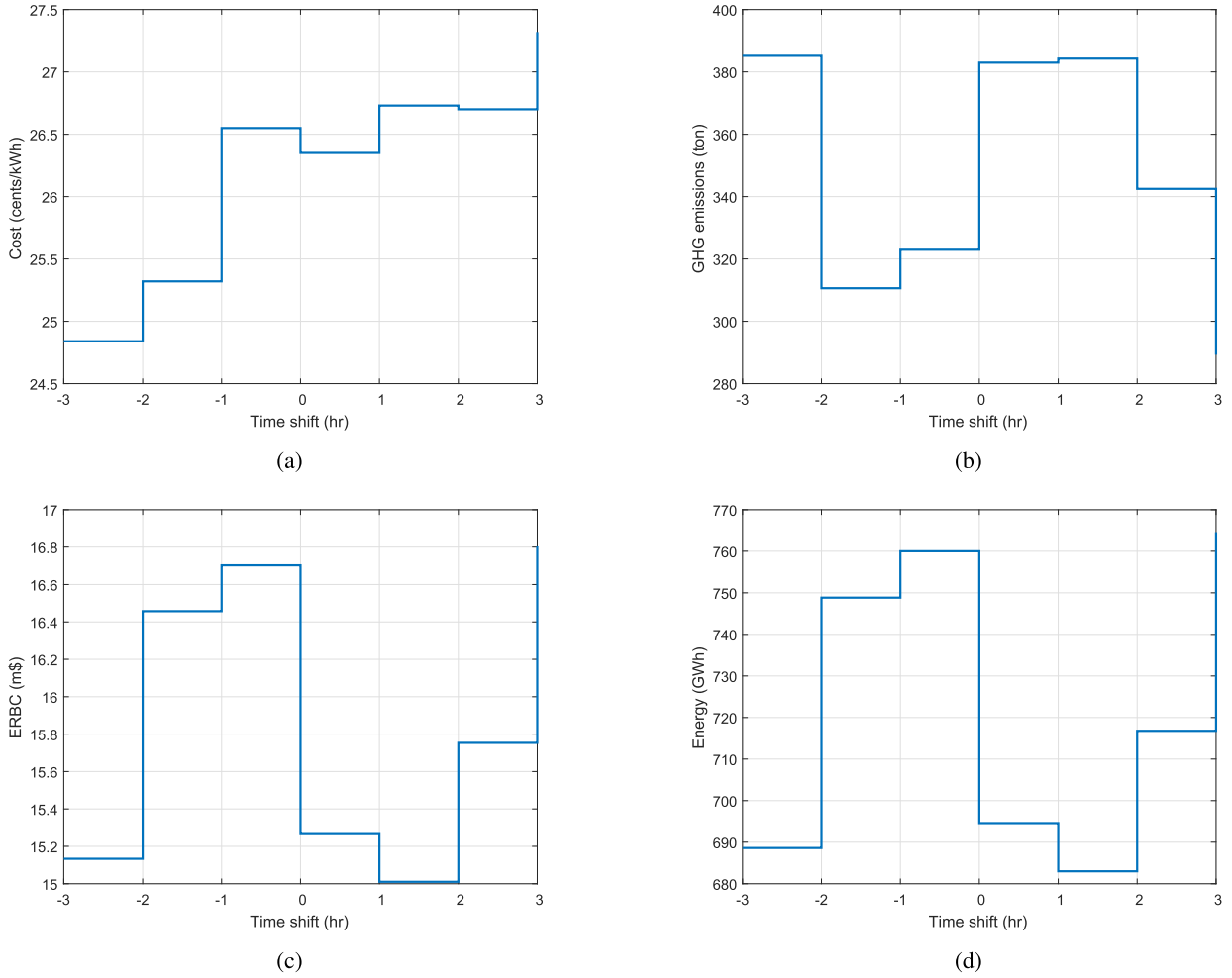

FIGURE 7. (a) Variation in cost per-unit w.r.t load shift (b) GHG emissions vs load shifting (c) ERBC vs load shifting (d) Clean energy served vs load shifting.

TABLE 5. Optimal capacities for different time shifts.

Shift (hr)	PV (MW)	WT (MW)	BESS (MWh)	BESS (MW)	DG (MW)
0	13.86	7.00	23.76	4.75	10.0
1	13.8	6.70	24.43	4.87	10.0
2	14.8	7.66	25.51	5.10	10.0
3	18.0	6.58	35.10	7.02	10.0
-1	20.0	4.40	32.24	6.45	9.00
-2	17.8	5.55	26.50	5.30	8.00
-3	14.6	6.12	16.55	3.30	8.00

minimum for a shift of 1 hour, as the installed capacities of RE sources and BESS are lowest for a shift of 1 hour.

The determination of the best time shift depends upon the priorities of the installing authority. If the priority is GHG emissions then the combination that corresponds to the shift of 3 hours can be taken as best solution. But if the the priority is the cost then the capacities of PV, WT, BESS, and DG corresponding to the shift of -3 can be taken as best solution. As the combination corresponding to -3 hours shift gives the lowest cost and supplies the load at 68% lesser emissions as compared to the conventional generation so it can be taken as best solution among the available options.

Sometimes it is difficult to shift the 100% of the load demand due to the presence of uncontrollable appliances. To study the impact of shifting different percentages of the total load demand on the installed capacities, cost, GHG emissions, ERBC, and clean energy served by the system, different percentages of the total load are shifted by -3 hours. The capacities that correspond to different percentages of load shifts are tabulated in Table 6.

The variation in per-unit cost with the different percentages of load shift is presented in Fig. 8a. It can be observed that cost is minimum for a shift of 60% of load and maximum for 20% of load shift. Even the shift of only 20% of the load by -3 hours can result in the considerable saving as compared to

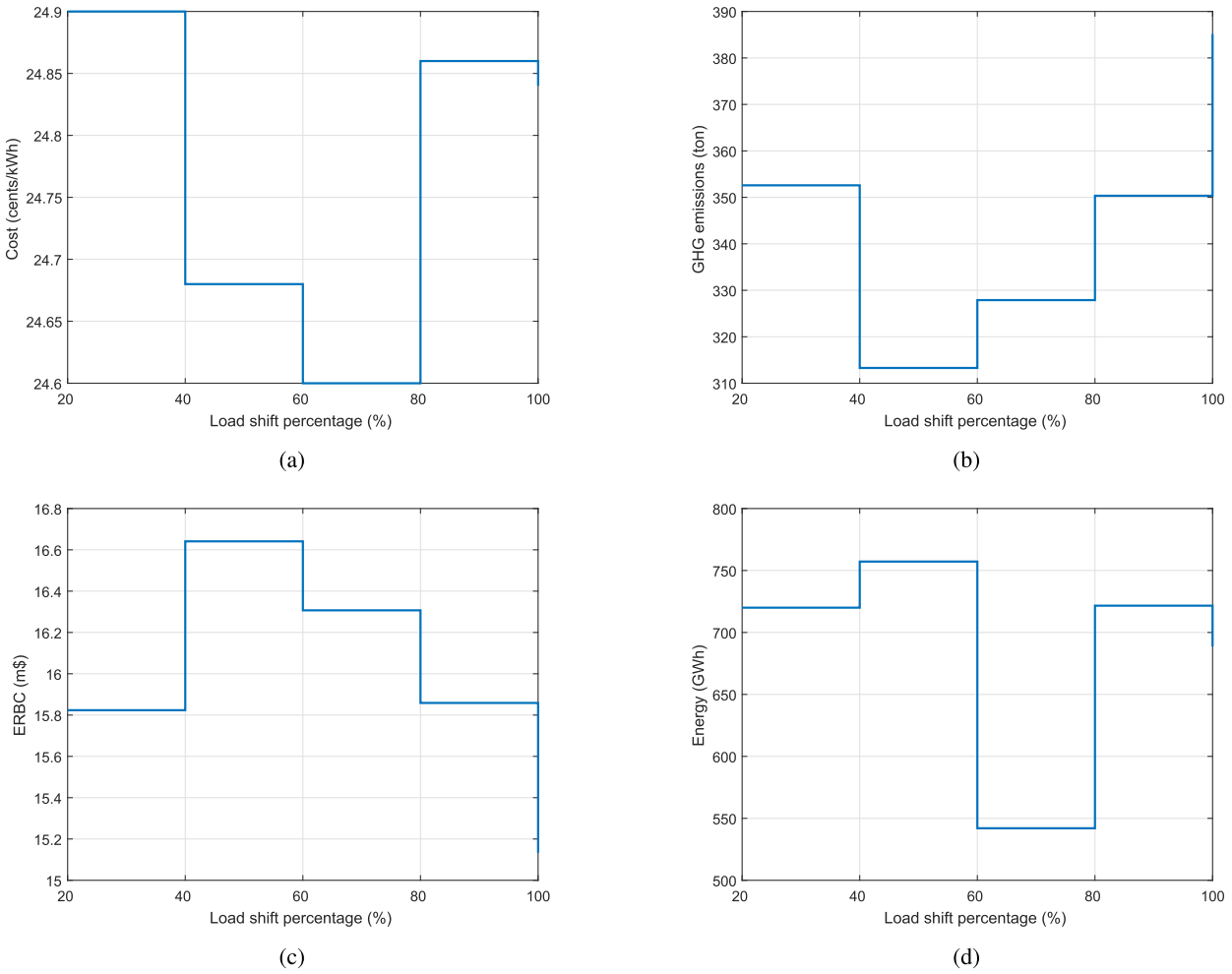

FIGURE 8. (a) Variation in cost per-unit w.r.t different percentages of load shift (b) GHG emissions vs percentages of load shift (c) ERBC vs percentages of load shift (d) Clean energy served vs percentages of load shift.

TABLE 6. Optimal capacities for different percentages of time shift.

Shift (%)	PV (MW)	WT (MW)	BESS (MWh)	BESS (MW)	DG (MW)
100	14.60	6.12	16.55	3.30	8.0
80	16.50	5.50	21.54	4.31	8.0
60	16.65	6.00	22.00	4.4	8.0
40	17.60	6.00	23.60	4.72	8.0
20	16.00	5.80	21.10	4.22	8.0

no shift. The variation in GHG emissions, ERBC, and clean energy supplied are shown in Fig. 8b, Fig. 8c, and Fig. 8d.

From the above analysis it can be concluded that shifting the load demand can result in cost reduction, GHG emissions reduction, savings in terms of ERBC and increase the green energy share. As it can be observed that shifting only 20% of the total load demand resulted in 5.5% reduction in per unit cost. It is important be noted that this reduction can actually result in huge savings as this is the reduction in one unit and this small system is serving more than 1000 GWh during its life time. Similarly, the GHG emissions are 7.9% lesser (as compared to no load shift) when 20% of the total load shifted by −3 hours. Moreover, it can be observed that shifting the load also benefits in terms of ERBC and clean energy served.

Any small residential community, cite office of a company, or even a single home can benefit from the proposed methodology. As the load control is easier in the aforementioned systems, proposed methodology can be utilized to get maximum benefits in terms of cost, GHG emissions, ERBC and clean energy. The proposed idea is also applicable for the large-scale power systems.

VII. CONCLUSION

An improved methodology for the capacity optimization of a typical residential MG employing distributed renewable generation, especially solar PV and wind, and conventional diesel generation coupled with battery energy storage system has been presented. The strategy is particularly focusing at the increased load demand from electric vehicles in addition to a residential house load. The capacity optimization

of six different topologies of renewable and conventional power mix along with storage technology, i.e., PV-WT-BES-DG, PV-WT-DG, WT-DG-BES, WT-DG, PV-BES-DG, and PV-DG has been done based upon the initial investment cost, replacement cost, operation cost, maintenance cost, dump energy cost, and GHG emissions. The multi-objective optimization problem is formulated and solved innovatively in the presence of various realistic constraints from RE sources generation system, BES system, diesel generation system, and EV load. A comparison has been made based on the cost per unit, GHG emissions, and ERBC, and it was observed that the proposed topology PV-WT-BESS-DG (see Section VI) is not only economical but also more reliable, has lesser emissions which makes it more environmental friendly, and higher ERBC.

Furthermore, the impact of load shifting on the cost, GHG emissions, ERBC and clean energy supplied by system has been investigated. It has been observed that shifting a small percentage (20%) of total load demand carefully can result in considerable cost savings (5.5% reduction in per-unit cost) and GHG emissions can be reduced significantly (7.9% reduction in GHG emissions). In particular, shifting the load demand can also increase ERBC and clean energy contribution in a MG system.

In future, considering V2G phenomenon of EVs, introducing uncertainty of EV owners, uncertainty associated with intermittent RE resources, and detailed ESS model including degrading and losses, can make the results more realistic.

ACKNOWLEDGEMENT

The authors would like to thank Research Institute (RI) at King Fahd University of Petroleum and Minerals and Saudi Electricity Company (SEC) for providing renewables and demand data to carry out this research. In particular, we appreciate the support of Mr. Hussain A. Al-Harthi for arranging time series data.

REFERENCES

[1] E. Kuznetsova, C. Ruiz, Y.-F. Li, and E. Zio, "Analysis of robust optimization for decentralized microgrid energy management under uncertainty," *Int. J. Electr. Power Energy Syst.*, vol. 64, pp. 815–832, Jan. 2015.

[2] U. Akram, M. Khalid, and S. Shafiq, "Optimal sizing of a wind/solar/battery hybrid grid-connected microgrid system," *IET Renew. Power Generat.*, vol. 12, no. 1, pp. 72–80, 2018.

[3] S. Chowdhury and P. Crossley, *Microgrids and Active Distribution Networks*. Stevenage, U.K.: Inst. Eng. Technol., 2009.

[4] Y.-S. Kim, E.-S. Kim, and S.-I. Moon, "Frequency and voltage control strategy of standalone microgrids with high penetration of intermittent renewable generation systems," *IEEE Trans. Power Syst.*, vol. 31, no. 1, pp. 718–728, Jan. 2016.

[5] Y. Kuang *et al.*, "A review of renewable energy utilization in islands," *Renew. Sustain. Energy Rev.*, vol. 59, pp. 504–513, Jun. 2016.

[6] L. A. de S. Ribeiro, O. R. Saavedra, S. L. de Lima, and J. G. de Matos, "Isolated micro-grids with renewable hybrid generation: The case of lençóis island," *IEEE Trans. Sustain. Energy*, vol. 2, no. 1, pp. 1–11, Jan. 2011.

[7] T. Ma, H. Yang, and L. Lu, "A feasibility study of a stand-alone hybrid solar–wind–battery system for a remote island," *Appl. Energy*, vol. 121, pp. 149–158, May 2014.

[8] M. Taylor, P. Ralon, and A. Ilas, "The power to change: Solar and wind cost reduction potential to 2025," in *Proc. Int. Renew. Energy Agency (IRENA)*, 2016, pp. 1–109.

[9] H. Abu-Rub, M. Malinowski, and K. Al-Haddad, *Power Electronics for Renewable Energy Systems, Transportation and Industrial Applications*. Hoboken, NJ, USA; Wiley, 2014.

[10] X. Hu, C. Zou, C. Zhang, and Y. Li, "Technological developments in batteries: A survey of principal roles, types, and management needs," *IEEE Power Energy Mag.*, vol. 15, no. 5, pp. 20–31, Sep. 2017.

[11] M. Khalid, A. Ahmadi, A. V. Savkin, and V. G. Agelidis, "Minimizing the energy cost for microgrids integrated with renewable energy resources and conventional generation using controlled battery energy storage," *Renew. Energy*, vol. 97, pp. 646–655, Nov. 2016.

[12] A. Khatamianfar, M. Khalid, A. V. Savkin, and V. G. Agelidis, "Improving wind farm dispatch in the australian electricity market with battery energy storage using model predictive control," *IEEE Trans. Sustain. Energy*, vol. 4, no. 3, pp. 745–755, Jul. 2013.

[13] A. V. Savkin, M. Khalid, and V. G. Agelidis, "A constrained monotonic charging/discharging strategy for optimal capacity of battery energy storage supporting wind farms," *IEEE Trans. Sustain. Energy*, vol. 7, no. 3, pp. 1224–1231, Jul. 2016.

[14] X. Wu, X. Hu, X. Yin, C. Zhang, and S. Qian, "Optimal battery sizing of smart home via convex programming," *Energy*, vol. 140, pp. 444–453, Dec. 2017.

[15] X. Lin and Y. Lei, "Coordinated control strategies for SMES-battery hybrid energy storage systems," *IEEE Access*, vol. 5, pp. 23452–23465, 2017.

[16] X. Dui, G. Zhu, and L. Yao, "Two-stage optimization of battery energy storage capacity to decrease wind power curtailment in grid-connected wind farms," *IEEE Trans. Power Syst.*, 2017, doi: 10.1109/TPWRS.2017.2779134.

[17] S. C. Davis, S. E. Williams, and R. G. Boundy, "Transportation energy data book: Edition 35," Oak Ridge Nat. Lab. (ORNL), Oak Ridge, TN, USA, Tech. Rep., 2016.

[18] S. Shafiq, M. A. Aslam, M. Khalid, A. Raza, and U. Akram, "Implementation of electric drive system using induction motor for traction applications," in *Proc. 6th Int. Conf. Clean Electr. Power (ICCEP)*, 2017, pp. 673–677.

[19] T. Sousa, H. Morais, Z. Vale, P. Faria, and J. Soares, "Intelligent energy resource management considering vehicle-to-grid: A simulated annealing approach," *IEEE Trans. Smart Grid*, vol. 3, no. 1, pp. 535–542, Mar. 2012.

[20] A. Y. Saber and G. K. Venayagamoorthy, "Resource scheduling under uncertainty in a smart grid with renewables and plug-in vehicles," *IEEE Syst. J.*, vol. 6, no. 1, pp. 103–109, Mar. 2012.

[21] K. H. Youssef, "Power quality constrained optimal management of unbalanced smart microgrids during scheduled multiple transitions between grid-connected and islanded modes," *IEEE Trans. Smart Grid*, vol. 8, no. 1, pp. 457–464, Jan. 2017.

[22] S. Park, J. Lee, S. Bae, G. Hwang, and J. K. Choi, "Contribution-based energy-trading mechanism in microgrids for future smart grid: A game theoretic approach," *IEEE Trans. Ind. Electron.*, vol. 63, no. 7, pp. 4255–4265, Jul. 2016.

[23] A. A. Khan, M. H. Rehmani, and M. Reisslein, "Cognitive radio for smart grids: Survey of architectures, spectrum sensing mechanisms, and networking protocols," *IEEE Commun. Surveys Tuts.*, vol. 18, no. 1, pp. 860–898, 1st Quart., 2016.

[24] V. C. Gungor *et al.*, "Smart grid technologies: Communication technologies and standards," *IEEE Trans. Ind. Informat.*, vol. 7, no. 4, pp. 529–539, Nov. 2011.

[25] S. E. D. Coalition, "The demand response snap shot: The reality for demand response providers working in europe today," in *Proc. Smart Energy Demand Coalition*, 2011, pp. 1–48.

[26] J. M. Morales, A. J. Conejo, H. Madsen, P. Pinson, and M. Zugno, *Integrating Renewables in Electricity Markets: Operational Problems*, vol. 205. New York, NY, USA: Springer, 2013.

[27] C.-H. Lo and N. Ansari, "The progressive smart grid system from both power and communications aspects," *IEEE Commun. Surveys Tuts.*, vol. 14, no. 3, pp. 799–821, 3rd Quart., 2012.

[28] W. Kempton and J. Tomić, "Vehicle-to-grid power implementation: From stabilizing the grid to supporting large-scale renewable energy," *J. Power Sour.*, vol. 144, no. 1, pp. 280–294, 2005.

[29] T. Wu, Q. Yang, Z. Bao, and W. Yan, "Coordinated energy dispatching in microgrid with wind power generation and plug-in electric vehicles," *IEEE Trans. Smart Grid*, vol. 4, no. 3, pp. 1453–1463, Sep. 2013.

[30] X. Wu, X. Hu, Y. Teng, S. Qian, and R. Cheng, "Optimal integration of a hybrid solar-battery power source into smart home nanogrid with plug-in electric vehicle," *J. Power Sour.*, vol. 363, pp. 277–283, Sep. 2017.

[31] X. Wu, X. Hu, S. Moura, X. Yin, and V. Pickert, "Stochastic control of smart home energy management with plug-in electric vehicle battery energy storage and photovoltaic array," *J. Power Sour.*, vol. 333, pp. 203–212, Nov. 2016.
[32] X. Wu, X. Hu, X. Yin, and S. Moura, "Stochastic optimal energy management of smart home with PEV energy storage," *IEEE Trans. Smart Grid*, to be published.
[33] L. Xu, X. Ruan, C. Mao, B. Zhang, and Y. Luo, "An improved optimal sizing method for wind-solar-battery hybrid power system," *IEEE Trans. Sustain. Energy*, vol. 4, no. 3, pp. 774–785, Jul. 2013.
[34] M. Sharafi and T. Y. ELMekkawy, "Multi-objective optimal design of hybrid renewable energy systems using PSO-simulation based approach," *Renew. Energy*, vol. 68, pp. 67–79, Aug. 2014.
[35] M. Alsayed, M. Cacciato, G. Scarcella, and G. Scelba, "Multicriteria optimal sizing of photovoltaic-wind turbine grid connected systems," *IEEE Trans. Energy Convers.*, vol. 28, no. 2, pp. 370–379, Jun. 2013.
[36] G. Ma, G. Xu, Y. Chen, and R. Ju, "Multi-objective optimal configuration method for a standalone wind–solar–battery hybrid power system," *IET Renew. Power Generat.*, vol. 11, no. 1, pp. 194–202, 2016.
[37] A. Kamjoo, A. Maheri, A. M. Dizqah, and G. A. Putrus, "Multi-objective design under uncertainties of hybrid renewable energy system using NSGA-II and chance constrained programming," *Int. J. Electr. Power Energy Syst.*, vol. 74, pp. 187–194, Jan. 2016.
[38] R. Dufo-López, I. R. Cristóbal-Monreal, and J. M. Yusta, "Optimisation of PV-wind-diesel-battery stand-alone systems to minimise cost and maximise human development index and job creation," *Renew. Energy*, vol. 94, pp. 280–293, Aug. 2016.
[39] J. Chen *et al.*, "Optimal sizing for grid-tied microgrids with consideration of joint optimization of planning and operation," *IEEE Trans. Sustain. Energy*, vol. 9, no. 1, pp. 237–248, Jan. 2018.
[40] C. S. Lai and M. D. McCulloch, "Sizing of stand-alone solar PV and storage system with anaerobic digestion biogas power plants," *IEEE Trans. Ind. Electron.*, vol. 64, no. 3, pp. 2112–2121, Mar. 2017.
[41] T. Dragičević, H. Pandžić, D. Škrlec, I. Kuzle, J. M. Guerrero, and D. S. Kirschen, "Capacity optimization of renewable energy sources and battery storage in an autonomous telecommunication facility," *IEEE Trans. Sustain. Energy*, vol. 5, no. 4, pp. 1367–1378, Oct. 2014.
[42] A. S. O. Ogunjuyigbe, T. R. Ayodele, and O. A. Akinola, "Optimal allocation and sizing of PV/Wind/Split-diesel/Battery hybrid energy system for minimizing life cycle cost, carbon emission and dump energy of remote residential building," *Appl. Energy*, vol. 171, pp. 153–171, Jun. 2016.
[43] M. H. Moradi, M. Eskandari, and S. M. Hosseinian, "Operational strategy optimization in an optimal sized smart microgrid," *IEEE Trans. Smart Grid*, vol. 6, no. 3, pp. 1087–1095, May 2015.
[44] A. Kaabeche, S. Diaf, and R. Ibtiouen, "Firefly-inspired algorithm for optimal sizing of renewable hybrid system considering reliability criteria," *Solar Energy*, vol. 155, pp. 727–738, Oct. 2017.
[45] L. Che, X. Zhang, M. Shahidehpour, A. Alabdulwahab, and Y. Al-Turki, "Optimal planning of loop-based microgrid topology," *IEEE Trans. Smart Grid*, vol. 8, no. 4, pp. 1771–1781, Jul. 2017.
[46] V. Kalkhambkar, R. Kumar, and R. Bhakar, "Joint optimal allocation methodology for renewable distributed generation and energy storage for economic benefits," *IET Renew. Power Generat.*, vol. 10, no. 9, pp. 1422–1429, 2016.
[47] F. S. Gazijahani and J. Salehi, "Stochastic multi-objective framework for optimal dynamic planning of interconnected microgrids," *IET Renew. Power Generat.*, vol. 11, no. 14, pp. 1749–1759, 2017.
[48] U. Akram, M. Khalid, and S. Shafiq, "An innovative hybrid wind-solar and battery-supercapacitor microgrid system—Development and optimization," *IEEE Access*, vol. 5, pp. 25897–25912, 2017.
[49] S. Kahrobaee, S. Asgarpoor, and W. Qiao, "Optimum sizing of distributed generation and storage capacity in smart households," *IEEE Trans. Smart Grid*, vol. 4, no. 4, pp. 1791–1801, Dec. 2013.
[50] A. Arabali, M. Ghofrani, M. Etezadi-Amoli, and M. S. Fadali, "Stochastic performance assessment and sizing for a hybrid power system of solar/wind/energy storage," *IEEE Trans. Sustain. Energy*, vol. 5, no. 2, pp. 363–371, Apr. 2014.
[51] L. Göransson, S. Karlsson, and F. Johnsson, "Integration of plug-in hybrid electric vehicles in a regional wind-thermal power system," *Energy Policy*, vol. 38, no. 10, pp. 5482–5492, 2010.
[52] Q. Zhang, T. Tezuka, K. N. Ishihara, and B. C. Mclellan, "Integration of PV power into future low-carbon smart electricity systems with EV and HP in Kansai area, Japan," *Renew. Energy*, vol. 44, pp. 99–108, Aug. 2012.
[53] N. Juul and P. Meibom, "Optimal configuration of an integrated power and transport system," *Energy*, vol. 36, no. 5, pp. 3523–3530, 2011.
[54] C. K. Ekman, "On the synergy between large electric vehicle fleet and high wind penetration—An analysis of the Danish case," *Renew. Energy*, vol. 36, no. 2, pp. 546–553, 2011.
[55] R. Atia and N. Yamada, "Sizing and analysis of renewable energy and battery systems in residential microgrids," *IEEE Trans. Smart Grid*, vol. 7, no. 3, pp. 1204–1213, May 2016.
[56] S. X. Chen, H. B. Gooi, and M. Q. Wang, "Sizing of energy storage for microgrids," *IEEE Trans. Smart Grid*, vol. 3, no. 1, pp. 142–151, Mar. 2012.
[57] R. Deng, Z. Yang, J. Chen, N. R. Asr, and M.-Y. Chow, "Residential energy consumption scheduling: A coupled-constraint game approach," *IEEE Trans. Smart Grid*, vol. 5, no. 3, pp. 1340–1350, May 2014.
[58] C. M. Colson and M. H. Nehrir, "Comprehensive real-time microgrid power management and control with distributed agents," *IEEE Trans. Smart Grid*, vol. 4, no. 1, pp. 617–627, Mar. 2013.
[59] B. Zhao, X. Zhang, P. Li, K. Wang, M. Xue, and C. Wang, "Optimal sizing, operating strategy and operational experience of a stand-alone microgrid on dongfushan island," *Appl. Energy*, vol. 113, pp. 1656–1666, Jan. 2014.
[60] X. Luo, J. Wang, M. Dooner, and J. Clarke, "Overview of current development in electrical energy storage technologies and the application potential in power system operation," *Appl. Energy*, vol. 137, pp. 511–536, Jan. 2015.

UMER AKRAM (S'16) received the B.Sc. degree (Hons.) in electrical engineering from the COMSATS Institute of Information Technology, Abbottabad, Pakistan, in 2013. He is currently pursuing the M.S. degree in electrical engineering from the King Fahd University of Petroleum and Minerals, Dhahran, Saudi Arabia. His current research interests include modern power system planning, operation and design, optimization and control of distributed energy resources, and renewable energy and energy storage systems.

MUHAMMAD KHALID (M'09) received the Ph.D. degree in electrical engineering from the School of Electrical Engineering and Telecommunications (EE&T), University of New South Wales (UNSW), Sydney, Australia, in 2011. He was a Post-Doctoral Research Fellow for three years and then he continued as a Sr. Research Associate with the School of EE&T, Australian Energy Research Institute, UNSW for another two years. He is currently an Assistant Professor with Electrical Engineering Department, King Fahd University of Petroleum and Minerals, Dhahran, Saudi Arabia. He has authored/co-authored several journal and conference papers in the field of control and optimization for renewable power systems. In addition, he has been a reviewer for numerous international journals and conferences. His current research interests include the optimization and control of battery energy storage systems for large-scale grid-connected renewable power plants (particularly wind and solar), distributed power generation and dispatch, hybrid energy storage, EVs, and smart grids. He was a recipient of the highly competitive Post-Doctoral Writing Fellowship from UNSW in 2010.

SAIFULLAH SHAFIQ received the B.Sc. degree in electrical engineering from the University of Engineering and Technology, Lahore, Pakistan, in 2014. He is currently pursuing the M.S. degree in electrical engineering from the King Fahd University of Petroleum and Minerals, Dhahran, Saudi Arabia. His current research interests include power system planning, renewable energy resources, electric vehicles, and power electronics.